Master's Degree Thesis
ISRN: BTH-AMT-EX--2005/D-17--SE

Correlation of a FE-model of a Truck Heat Exchanger with EMA

Varadarajan Sureshram

Department of Mechanical Engineering
Blekinge Institute of Technology
Karlskrona, Sweden
2005

Supervisor: Kjell Ahlin, Professor Mech. Eng.

Correlation of a FE-model of a Truck Heat Exchanger with EMA

Varadarajan Sureshram

Department of Mechanical Engineering

Blekinge Institute of Technology

Karlskrona, Sweden

2005

Thesis submitted for completion of Master of Science in Mechanical Engineering with emphasis on Structural Mechanics at the Department of Mechanical Engineering, Blekinge Institute of Technology, Karlskrona, Sweden.

Abstract:

A simplified FE-model of the subcomponent of the Charge air cooler – core is modelled using homogenisation technique. Modal testing was performed on the physical model of the same. On comparing the resonance frequencies of the test data (reference result) with FE-model data, the FE-model is reconciled and correlated.

Keywords:

FEA, CAC-core, Homogenisation, EMA, MIMO, Resonance frequency, Mode shapes, Correlation.

Acknowledgements

This work was carried out at Valeo Engine Cooling AB, Sölvesborg, Sweden under the supervision of Professor Kjell Ahlin from the University and Dynamics Manager, Anders Brorsson from the company, between September 2004 and April 2005.

I wish to express my sincere appreciation to my supervisors Professor Kjell Ahlin and Anders Brorsson for their professional engagement and guidance for the accomplishment of the thesis work. I wish to thank supervisor Anders Brorsson for his valuable cooperation and support.

I would also like to acknowledge Test Engineer Magnus Carlsson for installing software and all the staffs of the Test Lab Centre, VEC for cheering me during this period.

Last but not least, I'm ever grateful to my beloved Father, Mr. Ramasamy Varadarajan and my family members.

Karlskrona, April 2005

Varadarajan Sureshram

Contents

Appendices

The above mentioned CD is enclosed only in the Authors and the company's copies of the report.

1 Notation

F	Force [N]
A	Area [mm^2]
L	Length [mm]
E	Young's modulus [MPa]
G	Shear modulus [MPa]
σ	Stress [MPa]
ε	Strain
γ	Shear strain
ν	Poisson's ratio
$[D]^{-1}$	Compliance matrix
$x(t), \dot{x}(t), \ddot{x}(t)$	Displacement, velocity and acceleration vectors at time t
$\{F\}$	Force vector or Input vector
$[B(s)]$	System impedance matrix
$[H(s)]$	Transfer function matrix
s	Laplace domain variable
ζ	Relative damping
$[A_r]$	Residue matrix of r^{th} mode
$\{y\}$	Modal vector
Q	Modal scaling factor
E_f	Force transducer sensitivity [mV/N]
$E_{\ddot{x}}$	Accelerometer sensitivity [mV/ms^{-2}]

Indices

UX	Translational DOF in X
UY	Translational DOF in Y
UZ	Translational DOF in Z
RotX	Rotational DOF in X
RotY	Rotational DOF in Y
RotZ	Rotational DOF in Z

Abbreviations

CAC	Charge Air Cooler
PD	Product Development
DOF	Degree Of Freedom
FEA	Finite Element Analysis
FE	Finite Element
PR	Poisson’s Ratio
EMA	Experimental Modal Analysis
FRF	Frequency Response Function
SIMO	Singe Input Multi Output
MIMO	Multi Input Multi Output
MIF	Mode Indicator Function
MAC	Modal Assurance Criterion

2 Introduction

2.1 Background

The Valeo Engine Cooling AB in Mjällby (VEC) develops and manufactures engine cooling system for trucks. The main component of a cooling system is the heat exchanger such as radiator, charger air cooler and condenser. During its lifetime the heat exchanger is exposed to many different loads of which vibrations and thermal shock are perhaps the most severe ones. The development, including validation of the product is therefore extensive both in terms of coasts and lead-time. Hence, it is of interest to optimise the product due to structural strength and coasts already at an early stage of the product development process.

2.2 Purpose and limitations

The purpose of this thesis work is to:

1. Specify suitable measurement parameters for modal testing on CAC-core.
2. Construct, verify and validate a finite element model of a Charge Air Cooler (CAC) core with modal analysis.

The core normally includes tubes, turbolators, fins, header and side plates, all connected together by brazing joints. However due to time constraints, only the core without header and side plates were considered. Other limitations were that only tube bending modes of first order, including the first six modes, were correlated.

2.3 Methodology

The complex geometry of the turbolators inside the tubes and the fin does not allow for detailed modelling due to memory size on a standard PC. So these subcomponents are simplified using a method called homogenisation technique (discussed in chapter 3), which is an existing method developed by VEC.

To rely on the results of this simplified model, it needs to be verified and validated with data obtained from modal analysis, which involves the process of experimentally investigating the structure to obtain a modal

model description for dynamic behaviour. The emphasise lies on retrieving accurate measured data, which is influenced by a lot of factors. The quality of the data is of paramount importance in achieving a reliable FE-model.

FE-model validation is a logical procedure where we undergo an *iteration process* as shown in Figure 2.1., where the simulation results of the theoretical model (FE-model) are adjusted or corrected in order to bring its modal properties closer in acceptance with corresponding experimental data. Here the degree of acceptance depends on the purpose of the specific application. In this case comparison of resonance frequencies between test and FE- data is made. A difference of 5% is considered as the level of acceptance.

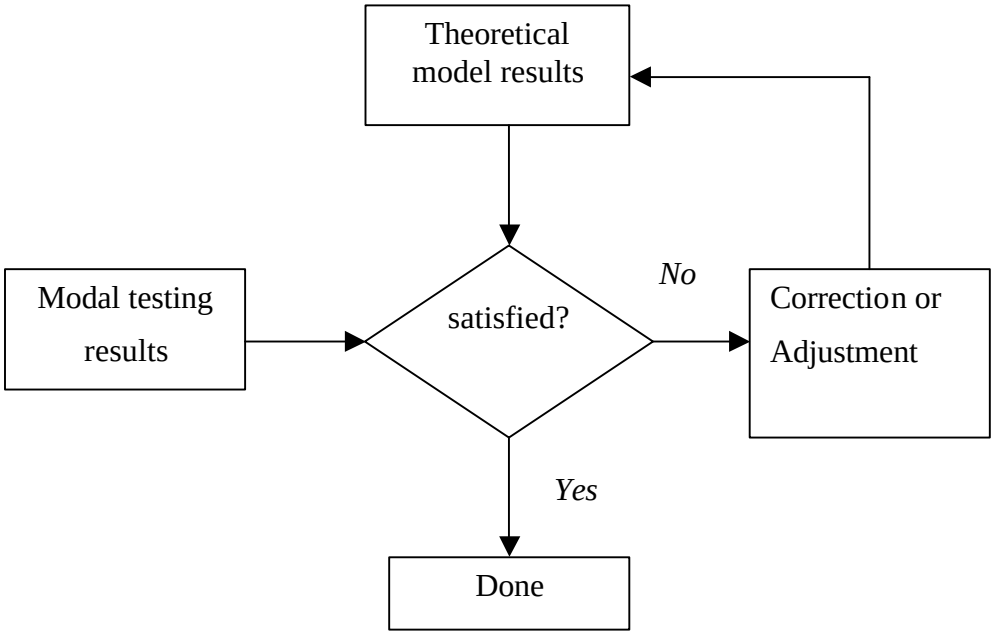

Figure 2.1, Iteration process

2.4 Thesis contribution

The contribution of this thesis work is measurement parameters for hammer & shaker testing and construction & correlation of a CAC-core FE model. This correlated Charge air cooler core is supposed to, when assembled into

a complete charge air cooler with tanks, headers and side plates, be used in an on-going fatigue prediction project at VEC.

3 FE-model optimisation using homogenisation technique

In FE-modelling of a structure, design optimisation is often considered. This chapter concerns with the procedure involved in optimisation, which concerns with simplifying a model by keeping the correct dynamic behaviour. The important objective of structural optimisation is to save pre-processing time and computer resources. When it comes to modelling heat exchangers this is especially important. A realistic geometrical representation of the core, including tubes, turbolators, fins, and brazing joints, is not possible since the model size would make it impossible to solve on a standard PC. Instead, the model which is being simulated has to be simplified to a greater extent provided that the exhibited characteristics of this model are accurate enough to represent the structural behaviour of the realistic model. For example, “Modelling flexible bellows by standard beam finite element”, by Broman, G. [1].

3.1 Methodology

The algorithm used here treats material property as design variable. The purpose of this algorithm, known as homogenisation, is to transform the realistic FE-model to a representative equivalent model. The homogenisation technique, which was originally introduced by Bendsoe and Kikuchi (1988), is used to find the optimal distribution of material property in a given design region. As mentioned earlier, the method used here, which is explained below, derives from the method developed by VEC [4].

A symmetry portion of the realistic FE-model of the tube with turbolator and fin are selected. By applying suitable boundary conditions change of form in the structure is studied. This enables us to compute orthotropic material properties, which are then defined to the representative equivalent model, which is a block. It is interesting to picturize how the *transformation* works by considering optimisation of the fin as an example.

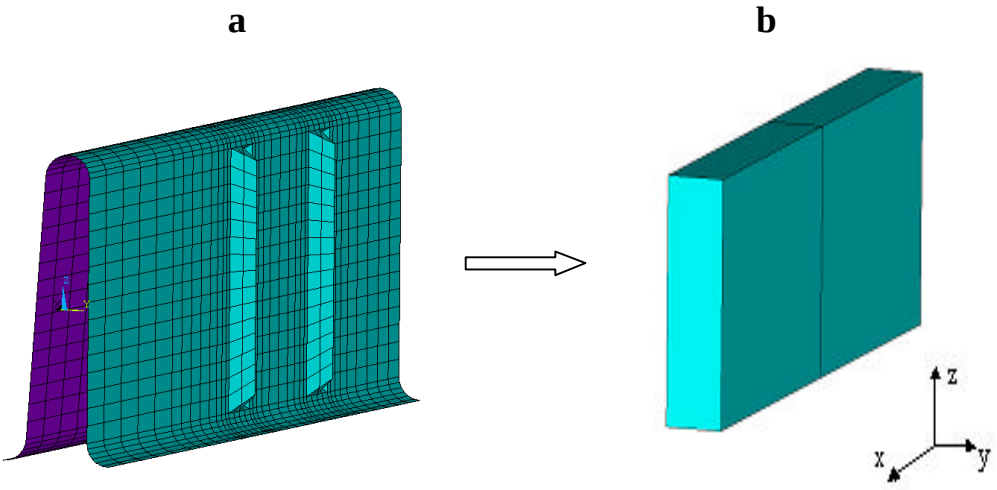

Figure 3.1 a, Realistic model of a period of fin (Shell elements).
b, Representative equivalent model (Solid element).

Here the realistic model is a symmetry portion of the fin, modelled by shell elements having a quadratic shape function. The material property used is the actual property, which is isotropic (same elastic properties in all directions). It is inferred from the above representation that the transformed model is no more elements (2354) but could be a *single element* of type solid185. Obviously the degrees of freedom are brought down to an optimum number, but still, with the aid of introducing orthotropic material properties (elastic properties differs in each of the three dimensions) the model will have similar elastic behaviour as the realistic model. Thus it demands the need for extracting orthotropic material properties from the model defined with isotropic material. The same analogy has been applied to tube plus turbolator and the turbolator alone.

3.2 Extraction of orthotropic material properties

3.2.1 Stress-strain relation

Stress is proportional to load and strain is proportional to deformation implying stress is proportional to strain. Hooke's law is the statement of that proportionality. As mentioned above orthotropic material properties are different in three mutually perpendicular directions at a point in the body

and further have three mutually perpendicular planes of material symmetry. So, as to enhance numerical computation the constitutive equation is normally expressed in matrix form as follows.

$$\{s\} = [D]\{e\} \tag{3.1}$$

where,

$\{s\}$= stress vector
$\{e\}$= strain vector
$[D]$= elasticity (stiffness) matrix and the inverse of this matrix is called the compliance matrix, which is given by

$$\{\varepsilon\} = [D]^{-1}\{\sigma\} \tag{3.2}$$

$$\begin{bmatrix} \varepsilon_x \\ \varepsilon_y \\ \varepsilon_z \\ \gamma_{xy} \\ \gamma_{yz} \\ \gamma_{zx} \end{bmatrix} = \begin{bmatrix} \frac{1}{E_x} & -\frac{\nu_{xy}}{E_x} & -\frac{\nu_{xz}}{E_x} & 0 & 0 & 0 \\ -\frac{\nu_{yx}}{E_y} & \frac{1}{E_y} & -\frac{\nu_{yz}}{E_y} & 0 & 0 & 0 \\ -\frac{\nu_{zx}}{E_z} & -\frac{\nu_{zy}}{E_z} & \frac{1}{E_z} & 0 & 0 & 0 \\ 0 & 0 & 0 & \frac{1}{G_{xy}} & 0 & 0 \\ 0 & 0 & 0 & 0 & \frac{1}{G_{yz}} & 0 \\ 0 & 0 & 0 & 0 & 0 & \frac{1}{G_{xz}} \end{bmatrix} \begin{bmatrix} \sigma_x \\ \sigma_y \\ \sigma_z \\ \tau_{xy} \\ \tau_{yz} \\ \tau_{zx} \end{bmatrix} \tag{3.3}$$

The compliance matrix must be positive definite [3] for ANSYS to solve and the matrix needs to be symmetric for a linear elastic behaviour of orthotropic material.

3.2.2 Implementation of boundary conditions

The homogenisation on the detailed description of the FE-model (tube + turbolator, turbolator alone and fin) has been treated as a three dimensional

elasticity problem, where in we have 15 unknown quantities which must be determined at every point in the body, namely, the 6 Cartesian components of stress, the 6 Cartesian components of strain and the 3 components of displacement. Due to assumptions in orthotropic property we have 9 independent elastic constants to determine, namely, $E_x, E_y, E_z, n_{xy}, \nu_{yz}, \nu_{xz}, G_{xy}, G_{yz}$ and G_{xz} [2]. Therefore the solution to this type of elasticity problem can be obtained by implementing boundary conditions in such a way to get the desired change of form in the structure. For example, boundary conditions specified to calculate Young's modulus in X-direction are discussed below,

In brief, this is a typical Type 1 boundary-value problem where in displacements are prescribed over entire boundary as loads [2], refer figure 3.2. As a matter of convenience a small value 0.1 *mm* is specified for the displacement. The condition *Coupled DOF (CP)* is applied on the selected plane shown in table (3.1). As a result of this coupling the nodes subjected to it are forced to take the same displacement in the specified nodal coordinate direction.

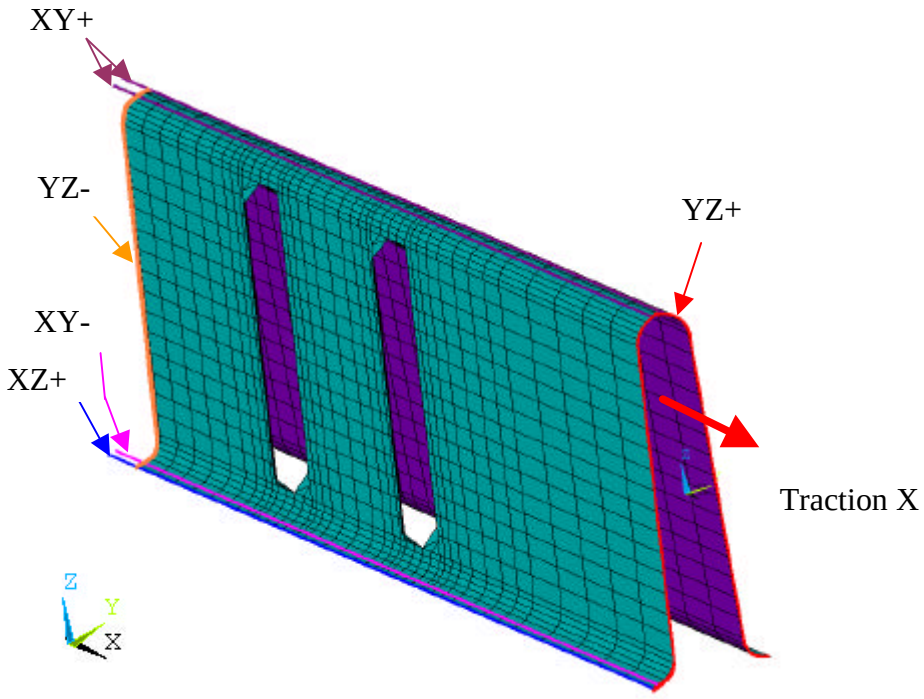

Figure 3.2, Boundary selection in Fin

Table 3.1, Boundary conditions applied for Traction X

Plane	UX	UY	UZ	RotX	RotY	RotZ	CP DOF
YZ+	0.1	-	-	-	-	-	-
YZ-	0	-	-	-	0	0	-
XZ+	-	-	-	0	-	0	CP(Y)
XZ-	-	0	-	0	-	0	-
XY+	-	-	-	-	-	-	CP(Z)
XY-	-	-	0	-	-	-	-

When a body subjected to system of loads exerts force in the direction of applied load (X-direction), the stress can be calculated by dividing the obtained reaction force by the area of the surface under consideration (YZ-). Similarly the engineering strain (the amount of stretch) can be obtained by taking the ratio of change in length to original length. Here on considering the plane normal to the X-axis, Young's modulus E_x can be computed by applying Hooke's law. It is natural that the structure will experience deformation in the directions (XZ+ & XY+) normal to the applied load, in this case both in y and z direction, by which the Poison's ratio ν_{xy} and ν_{xz} (the first subscript refers the direction of stretch and the second refers the direction of compression effected by the later) can be obtained as shown below. Similarly the rest of the orthotropic material properties are calculated both for fins and tube with turbolators by applying the suitable boundary conditions.

The results obtained from ANSYS on implementing the above boundary conditions and computed material properties from Traction in X are shown below.

Reaction structure force:

$$F_x = 344.66N$$

Deformation:

$$U_x = 0.1mm$$

$$U_y = 0.04413mm$$

$$U_z = 0.006112mm$$

1.) $E_x = \left(\frac{\sigma_x}{\varepsilon_{xx}}\right) = \frac{\left(\frac{F_x}{A - plane.yz}\right)}{\left(\frac{U_x}{L_x}\right)} = 2496.63 Mpa$

2.) $PR_{xy} = \left(\frac{e_{yy}}{e_{xx}}\right) = \frac{\left(\frac{U_y}{L_y}\right)}{\left(\frac{U_x}{L_x}\right)} = 4.01$

3.) $PR_{xz} = \left(\frac{e_{zz}}{e_{xx}}\right) = \frac{\left(\frac{U_z}{L_z}\right)}{\left(\frac{U_x}{L_x}\right)} = 0.1948$

3.3 Verification of extracted result

As discussed in the above section 3.2.2 the structure experiences deformation in directions normal to the applied load, so when on applying boundary conditions to force the structure to have traction in X-direction we also determine Poisson's ratio (ν_{xy}, ν_{xz}) in both the directions. The compliance matrix formed by the extracted orthotropic material properties are checked for its (I) determinant value, which in our case is greater than zero and (II) the symmetry in the matrix is checked for linear elastic behaviour. To have symmetry the following conditions should be satisfied.

$$\nu_{yx} = \nu_{xy} \times \frac{E_y}{E_x} \qquad 3.4$$

$$\nu_{zx} = \nu_{xz} \times \frac{E_z}{E_x} \qquad 3.5$$

$$\nu_{zy} = \nu_{yz} \times \frac{E_z}{E_y} \qquad 3.6$$

The terminology traction indicates the drawing action. The verified results are produced in tabular format in Appendix A. Based on the results (I) and (II) this approach for optimisation of theoretical modelling is considered as verified.

4 Model in ANSYS

4.1 Creating parametric model

The CAC core is modelled using APDL - *ANSYS Parametric Design Language* - a scripting language that we can use to automate repetitive tasks. Using APDL for modelling allows generic model to be built. Such models are of significant advantage if a series of analysis are to be performed. It makes possible to set up table of values, or to pass arguments to a macro (i.e. itemized codes) by which geometry, material properties or boundary conditions can be influenced. The *scope* of this parametric modelling is that it saves time and enhances optimum resource use in PD.

4.2 Physical model of core

The physical model of core encompasses tubes, turbolators and fins as shown in Figure 4.1.

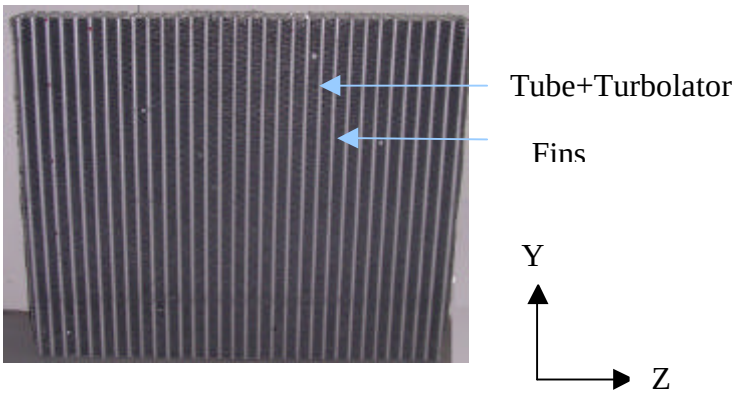

Figure 4.1, Physical model of core.

When it comes to modelling, repetitive tasks are always perfect candidates for automation. Design automation is feasible with the availability of a wide range of features in ANSYS.

4.3 Modelling of core

A macro has been written which drives ANSYS in the process from model build up to solving. The macro enters the pre-processor and initializes key points for tube geometry, which are then used to generate the area, where

this area is meshed to generate shell elements forming the outer geometry of the tube. These shell elements have been generated only for the sake of extruding it to obtain solid elements for the tube plus turbolator, which are defined by orthotropic material properties. In the same way solid elements of fin are generated. Now the generated symmetry portions of tube plus turbolator & fin are reflected to generate the full length of the parts. At this stage the shell elements, which are used for extrusion, are cleared off from the model. The full length tube, including turbolator, and fin are then allowed to generate the rest of the core. With this completed FE-model of the core the macro enters the solution phase by specifying to solve for modal analysis using Block Lanczos method in the frequency range 5-1000 Hz.

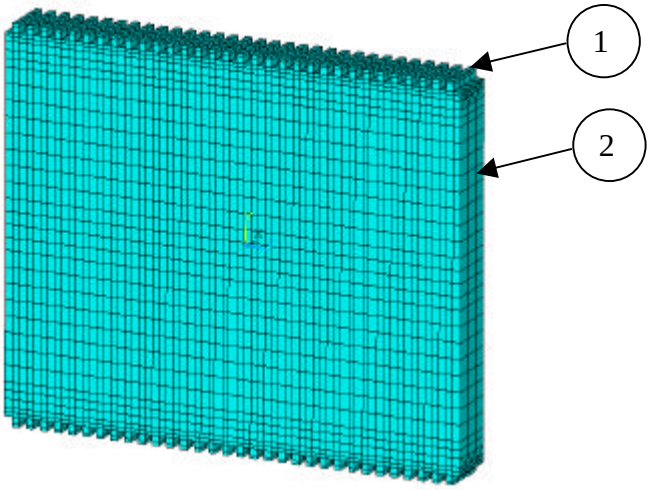

Figure 4.2, FE-model of core

1. Simplified representation of Tube+Turbolator (homogenised)
2. Simplified representation of Fin (homogenised)

5 Modal analysis theory

The vibration behaviour of the structure should be studied experimentally in order to have a precise identification and know-how of the dynamic characteristics, namely natural frequencies (resonant frequencies), mode shapes (deformation pattern) and damping. These are the characteristics which depend on the weight and stiffness of a structure and might affect the response due to excitation.

The phenomenon, *Resonance*, occurs when a structure excited at a frequency that coincides with the natural frequency of the structure. These are the frequencies that a structure will select if allowed vibrating freely without any excitation. For each of these natural frequencies there exists a specific deformation pattern, the so-called mode shapes [5]. At resonance the amplitude of the response increases dramatically, which can be restricted by the damping present in the structure. Continued vibration at resonance may result in fatigue.

The experimentation stated above often refers to the type of test that is generally made under much more closely controlled conditions, which gives more accurate and detailed information. This type of test that includes both data acquisition and its subsequent analysis giving the dynamic properties is termed Modal Testing and popularly as Experimental Modal Analysis or EMA. Ultimately, this gives the mathematical description of dynamic or vibration behaviour of the structure.

In the following section solution for an undamped unforced system and relation between FRF and modal vector is described.

5.1 Solution for undamped unforced system

The equation of motion for a multiple degree of freedom system is given by

$$[M]\left\{\ddot{x}(t)\right\}+[C]\left\{\dot{x}(t)\right\}+[K]\left\{x(t)\right\}=\{F(t)\} \qquad (5.1)$$

In the above equation we have mass matrix [M], a diagonal matrix, and symmetry matrices [C], damping matrix, and stiffness matrix [K]. The off-diagonal elements of [M] and [K] matrices show the degree of coupling.

The solution for a second order, linear, time invariant system begins often with an undamped system ([C] = 0). The system of equations in (5.1) is then reduced as

$$[\mathrm{M}]\{\ddot{\mathrm{x}}\} + [\mathrm{K}]\{\mathrm{x}\} = \{\mathrm{F}\} \tag{5.2}$$

For brevity notation t is dropped. Now considering free solution (unforced), which means that the forcing function is zero.

$$\{\mathrm{F}\} = 0 \tag{5.3}$$

The general solution from the theory of calculus for equation (5.1) is known as,

$$\{x\} = \{X\}e^{lt} \tag{5.4}$$

Here l is the complex valued frequency given by $l = s + jw$. With equations (5.3) & (5.4), equation (5.1) becomes

$$\left(l^2[M] + [K]\right)\{X\} = 0 \tag{5.5}$$

To obtain non-trivial solution to the above equation, the determinant should be set to zero and on rewriting to decouple the system equation gives

$$\left(\det\left|[M]^{-1}[K] + l^2[I]\right|\right)\{X\} = 0 \tag{5.6}$$

The equation (5.6) is a polynomial equation whose roots give the eigenfrequencies (natural frequencies). The vector $\{\mathrm{X}\}$ that satisfies the equation (5.6) for the corresponding eigenfrequency is the eigenvector or mode shape vector $\{\psi_r\}$.

5.2 FRF in relation to modal vectors

The FRF, frequency response function, measured during modal testing is actually the system transfer function (ratio of output response of a structure due to applied force) evaluated along the frequency axis. On applying the Laplace transform on equation (5.1) and with assuming initial conditions (displacement, velocity) are zero, the following algebraic equation results.

$$\left[s^2[M]+s[C]+[K]\right]\{X(s)\}=\{F(s)\} \tag{5.7}$$

The matrix in the left side of the above equation is termed the system impedance matrix or system matrix $[B(s)]$ [10], which is also symmetric due to the properties of matrices associated in equation (5.1), giving (5.7) as

$$[B(s)]\{X(s)\}=\{F(s)\} \tag{5.8}$$

The system transfer function is defined as the inverse of system impedance matrix, that is

$$[B(s)]^{-1}=[H(s)] \tag{5.9}$$

Pre-multiplying equation (5.8) by $[B(s)]^{-1}$ and with (5.9) yields

$$[H(s)]\{F(s)\}=\{X(s)\} \tag{5.10}$$

The above equation shows that system response $\{X(s)\}$ relates to the system forcing function $\{F(s)\}$ through system transfer function matrix $[H(s)]$.

In equation (5.9) the inverse of the system matrix is known by dividing its adjoint matrix by the determinant of the matrix giving

$$[B(s)]^{-1}=\frac{Adj[B(s)]}{\det|B(s)|}=[H(s)] \tag{5.11}$$

The element of transfer function matrix $[H(s)]$ can be expanded by its partial fraction. If we consider the first element of the first row, we obtain

$$H_{11}(s)_{s=j\omega}=\sum_{r=1}^{N}\frac{A_{11r}}{s-\lambda_r}+\frac{A^*_{11r}}{s-\lambda^*_r} \tag{5.12}$$

In the above equation the element A^*_{11r} is the complex conjugate of A_{11r}. For the whole system, the $[H(s)]$ matrix is given by

$$[H(s)]_{s=jw}=\sum_{r=1}^{N}\frac{[A_r]}{s-l_r}+\frac{[A^*_r]}{s-l^*_r} \tag{5.13}$$

Here, N is the number of interested modes and l_r is the system pole, which is given by

$$l_r = -z_r w_r \pm j w_r \sqrt{1 - z_r^2} \tag{5.14}$$

where

w_r = undamped resonance frequency of mode r and

z_r = relative damping of mode r

The term $[A_r]$ is the residue matrix, which gives the mode shapes.

$$[A_r] = Q_r \{y\}_r \{y\}_r^T \tag{5.15}$$

It is inferred from the above equation (5.15) that the element of the residue matrix is a term comprising scaling factor Q_r times the value of mode shapes that is the product of vectors $\{\psi\}_r \{\psi\}_r^T$, measured at response and input point (considering as the reference point), respectively.

6 Modal Testing

To practice modal testing is an art, to prepare for modal testing is a science. Here science refers in preparing a composite stuff like paint, tedious and time consuming. Where as art refers painting a house, rather fast, easy, and interesting too. Here vibration testing is performed for modal analysis, the simultaneous measurement of both excitation and response of the tested structure.

The influences either by the support, the excitation equipment or the transducers on dynamic behaviour of the structure under test should be realised. The test preparations are made based on this to obtain the data, sets of FRF, that are as close to the correct answer as required. That is the FRF obtained this way should be capable for extraction of accurate properties for all the modes of interest. The preliminary survey (SIMO) using hammer excitation was performed on core along with headers and side plates. During the actual testing both core with and without headers & side plates where tested.

6.1 Test planning and preparations

6.1.1 Support of the test structure

As the purpose of the modal test data is to update a FE-model, which should be reliable and satisfy the need, very extensive and high quality measurements are necessary. The quality of the data can be judged by reciprocity and repeatability [8]. Repeatability in a test can be achieved via free-free boundary condition, which is usually the best-satisfied condition unless the structure under test is a power station.

As the condition states, obviously, it is not possible to float the structure in air without any holding points. However suspending the structure can approximate this condition, though it poses negligible amount of constraints. The suspension material should be given due consideration, rubber chords, very flexible spring are few to mention, where the damping influenced by this on the structure are nominal. This approximation no longer yields rigid body modes (3 translation and 3 rotation modes) at zero frequency as they are supposed to be. But it is possible to accomplish rigid

body modes at very low frequency that is less than 10 – 20% of the first mode of interest. The rigid body modes appeared as condition stated above, which shows that the implemented suspension system is acceptable.

The support of the test structure approximating free-free boundary conditions is shown in Figure 6.1, where a rubber chord is used to suspend the structure via thin steel wire tied to the test structure. Reciprocity is discussed latter in sub section (6.3.2.1).

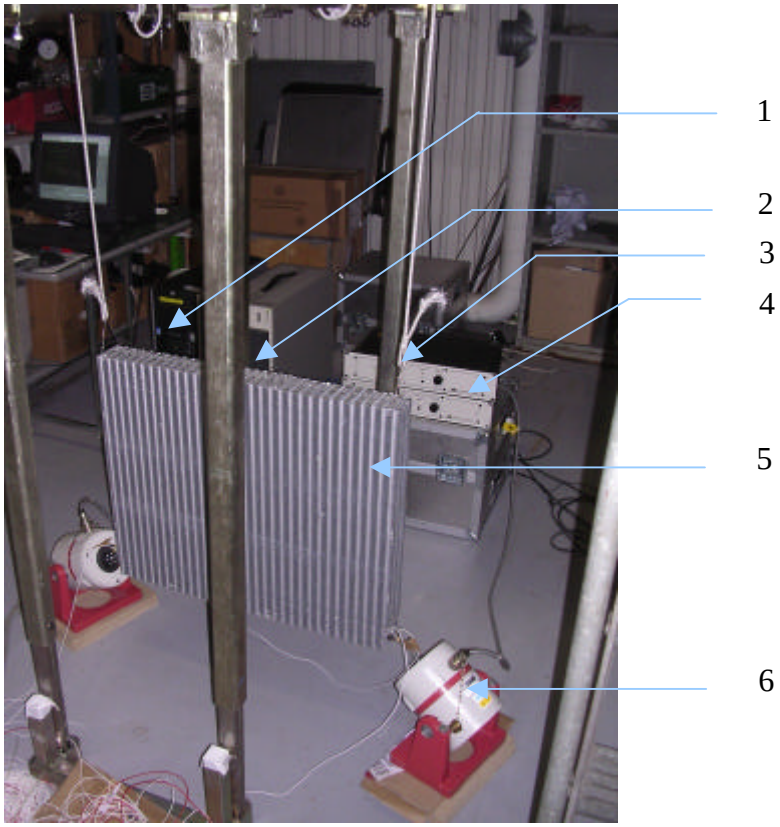

Figure 6.1, Measurement setup of Test Structure.

1. I-DEAS-Test software.
2. Measurement system HP VXI (Front end).
3. Flexible chord tied to steel wire.
4. Power amplifier.
5. Test structure-core without headers & side plates.
6. Grounded excitation (shaker).

6.1.2 Selection of reference point

The reference point is kept fixed through out the measurement. That is the point for excitation if shaker is used and point for accelerometer when hammer is used for exciting test structure. The foremost concern in selecting this fixed point is that it should not lie on a nodal point, zero displacement, for any of the modes of interest.

Here the test specimen resembles the rectangular plate (benchmark structure in modal analysis). Hence, the choice fell on the four corners as reference points. It is to be noted that in a complicated structure the deflection obtained in a specific direction might be low when compared to the other principle directions. For this ambiguous aspect the reference point should be put to distribute the excitation energy in all three principle directions for shaker testing. Here this is accomplished by an oblique angle excitation.

6.1.3 Selection of response point

The selection of response points means to select a set of adequate points such that these points are capable enough to uniquely distinguish each mode shape so as to avoid spatial aliasing. When a limited subset of response points are used this leads to an incomplete geometric definition and not an explicit representation of mode shapes.

6.1.4 Mounting of accelerometer

The most common methods for mounting accelerometers are screws, glue, wax, and magnet. The surface should be clean and smooth for mounting since a smallest bit of dirt or unevenness may give rise to elasticity, where the measurement can be influenced seriously as mounting resonance get lowered due to this. Here accelerometers are glued. To avoid mass loading, a rule of thumb in modal testing is that the mass of the accelerometers should be less than 10% of the apparent mass in the measurement point.

6.1.5 Accelerometer calibration

All the nine accelerometers used in measurement were already calibrated by Test Lab Centre in VEC by reference calibration method.

6.1.6 Force Transducer calibration

Calibration of the force transducer is performed by mass calibration, with the aid of an accurate known mass (.9816 kg). The calibrated accelerometer is attached to one side of the mass as shown in the Figure 6.2.

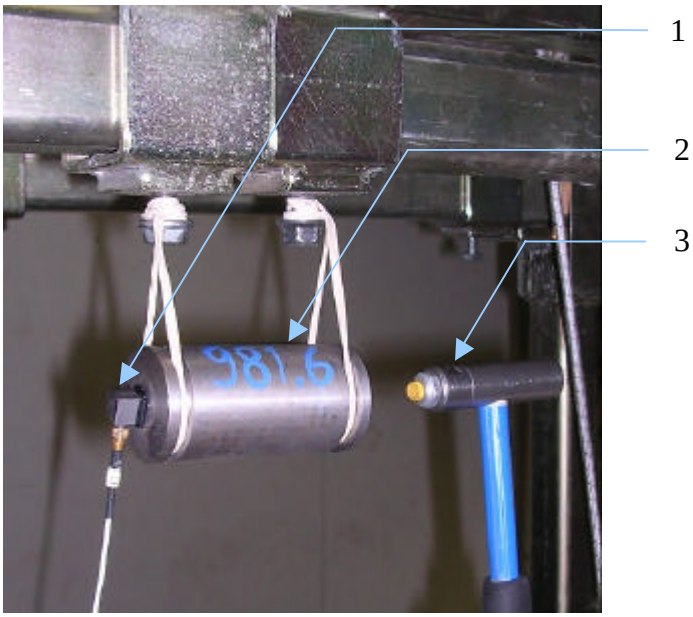

Figure 6.2, Calibration Setup.

1. Calibrated accelerometer.
2. Known mass.
3. Force transducer

The mass is gently tapped on the other side by the hammer and accelerance is measured, which is the ratio between response and force level. This gives a constant value 1/mass for all frequencies. Measured quantities are usually the ratios (Volts/volt) of accelerometer and force transducer. The measured amplitude in our case is 0.416 Volts/volt. These voltages (V) are related to the physical quantities being measured by the sensitivities (E) of the respective transducer which is given by

$$V_f = E_f * f \qquad (6.1)$$

$$V_{\ddot{x}} = E_{\ddot{x}} * \ddot{x} \qquad (6.2)$$

Now on dividing (6.2) by (6.1), we obtain

$$\frac{\ddot{x}}{f} = \left(\frac{V_{\ddot{x}}}{V_f}\right) * \left(\frac{E_f}{E_{\ddot{x}}}\right) \qquad (6.3)$$

In the above equation the ratios of the two sensitivities are taken as E, reducing the above equation to

$$\frac{\ddot{x}}{f} = \left(\frac{V_{\ddot{x}}}{V_f}\right) * E \qquad (6.4)$$

By Newton's Law, we have

$$\frac{\ddot{x}}{f} = \frac{1}{m} \qquad (6.5)$$

Equating the above two equations (6.4) and (6.5), we obtain the overall system calibration factor E.

$$E = \frac{1/m}{V_{\ddot{x}}/V_f} = \frac{1/.9816}{0.416} = 2.44$$

This factor is then used to compute the actual sensitivity of the force transducer, by dividing the assumed sensitivity value in our case 1000 mV/EU, giving the calibrated value for force transducer as 409.83 mV/EU.

6.2 Mobility Measurement

I-DEAS Test software has two tasks for data acquisition, namely

- Model preparation
- Signal processing

6.2.1 Model preparation

The wire frame model description of the test structure is created where the measurement points (MP) are defined as nodes (asterisk) and the geometry as elements, refer Figure 6.3.

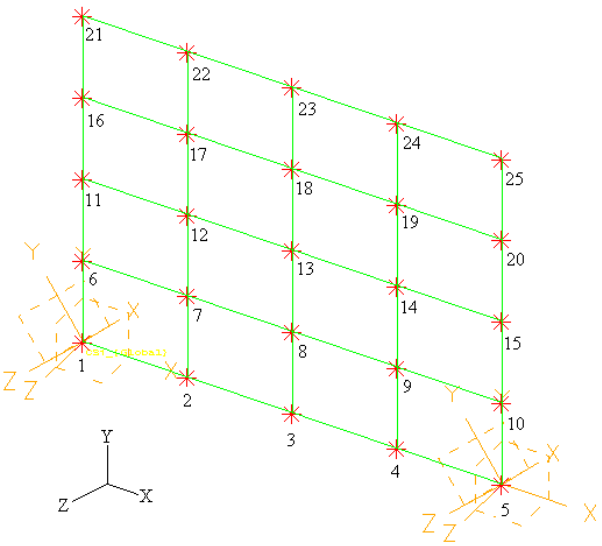

Figure 6.3, Model Geometry of test structure.

6.2.2 Signal processing

In the signal processing task standard measurement is used by initializing front end. Here the steps followed are calibrating front end, creating transducers, configuring channels, setting up channel table, preview followed with measurements, which are recorded as associated data files (ADF). This task performs averaging of stationary signals into FRFs, coherence functions, etc.

6.3 Preliminary survey

6.3.1 Single-Input Multi Output Testing (SIMO)

In order to realize the inherent problem on the structure to be tested, SIMO testing is carried out as a preliminary survey. Here only core with headers & side plates was considered. This is a single-point testing which comes under the category of Phase-Separation testing (all modes excited simultaneously), also called non-sinusoidal method [6]. Impact testing, in this case roving hammer test, is made as it is faster, cheaper and easier in preliminary survey of modal testing. The high resilience tip is used as the chosen frequency range is 0-400 Hz (mass and stiffness of test structure also contributes to this choice of tip), which would provide the sufficient excitation energy. The core is excited in Z-direction refer Figure 6.3, which produces a very short sharp peak approximating a Dirac delta function that has flat spectrum. A good excitation should be considerably flat (not more the 3 db roll-off) over the desired frequency range. So as to predict the closely spaced modes, three accelerometers, at different measurement points (3-corners of test structure), are used to sense the response acceleration in three principle directions, which reduces the risk that all references are placed on the nodal line for any of the modes and at least one FRF with good estimate is obtained. Following the initial measurement settings for impulse excitation [7], the final settings are tabulated, refer Table 6.1

Table 6.1, Measurement setting for hammer testing.

Parameters	Settings
Number of frequency lines	1601
Frequency span	400 Hz
Measurement time per block	4 Sec
Frequency resolution	0.25 Hz
Trigger settings	Every Frame level 10%
Number of Averages	3
Time window with parameters	Exponential Decay 30%

6.3.2 Quality check

The following quality checks discussed in the following sub sections where performed.

6.3.2.1 Reciprocity check

The property of Maxwell's Rule of Reciprocity, measured transfer FRF for a force at location j and a response at location i should correspond directly with the measured transfer FRF for a force at location i and response at location j, as shown in Figure 6.4.

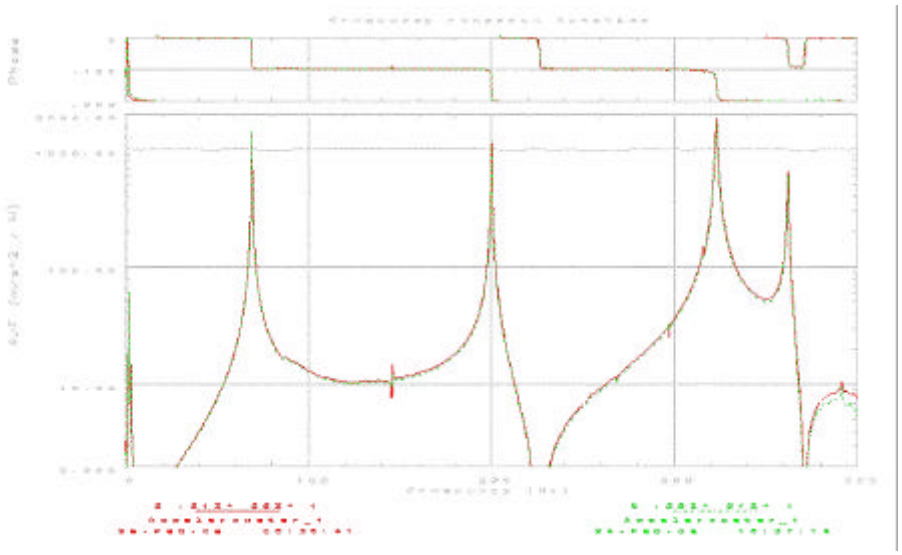

Figure 6.4, Overlaid transfer FRF shows reciprocity.

6.3.2.2 Drive point FRF

Drive point FRF, (direct FRF) where the input force and output response are measured at the same point and in the same direction, is characterised with antiresonance separating all the resonances. On inferring the phase it looses 180 degree of phase passing over a resonance and gain 180 degree of phase passing over antiresonance, where the peaks in the imaginary part of FRF must all point in the same direction, i.e. they should be either in phase or out of phase with each other as shown in Figure 6.5.

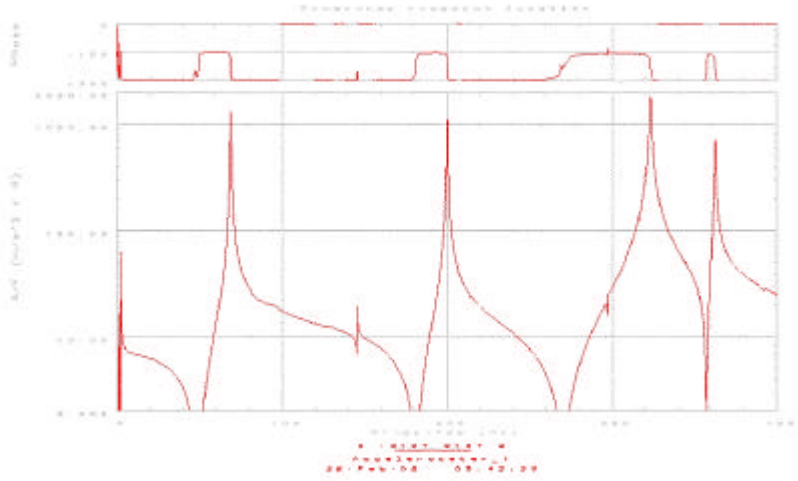

Figure 6.5, Drive point FRF

6.3.2.3 Mass loading

Mass Loading is checked by positioning a dummy accelerometer near the reference sensor and FRF is measured. Now again FRF is measured on removing the dummy sensor. Measured FRFs are overlaid as shown in Figure 6.6, where there is no shift in frequency, which shows that there is no effect of mass loading.

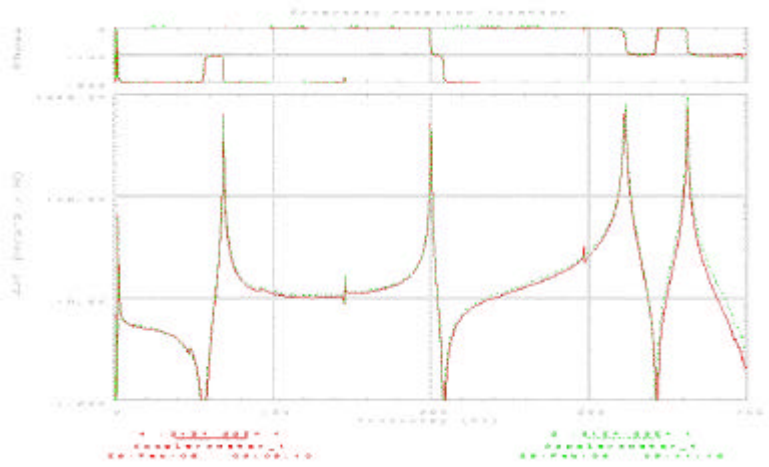

Figure 6.6, Overlaid FRF shows no effect of mass loading.

6.3.2.4 Linearity check

Linearity is checked using shaker excitation as this mode provides easy means on comparing with hammer excitation. Here two FRFs where measured with varied excitation level, i.e. during second measurement the force level is doubled. The FRFs are overlaid, it is inferred from the Figure 6.7 that there is no difference in amplitude, i.e. FRFs should be independent of excitation level for a linear structure.

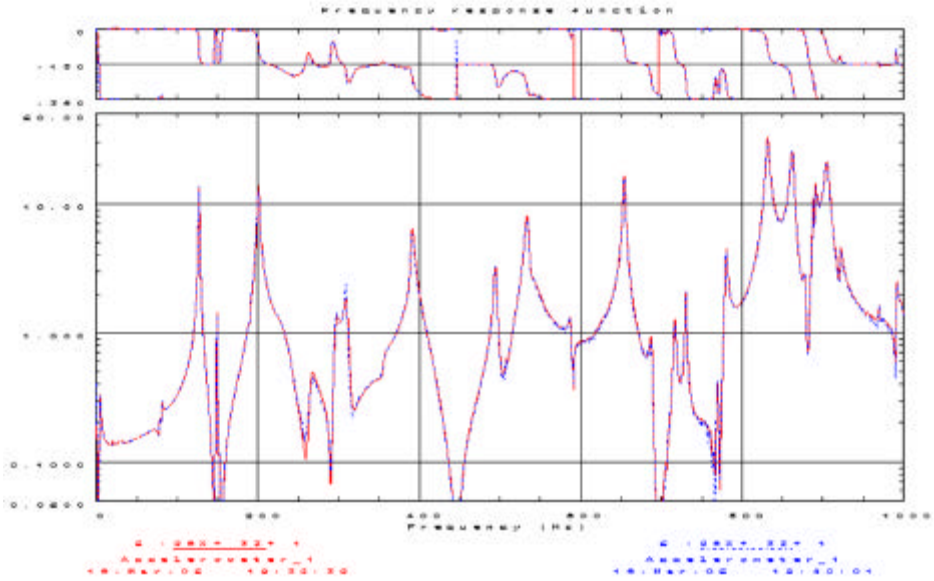

Figure 6.7, Overlaid FRF shows test structure's linearity.

6.3.3 Inference on preliminary survey

On exciting in Z-direction by considering 25 measurement points with reference placed in 1X, 21Z, and 25Y direction (refer Figure 6.3), three rows of FRF matrix elements is measured and the data's are curve fitted using Polyreference complex exponential method. The Multivariate MIF is shown in Figure 6.8 and the obtained mode shapes are shown in Table 6.2. We can observe mode #2 (145.47 Hz), mode #4 (206.75 Hz), mode #5 (296.88 Hz) that looks like operating deflection shape, uncharacteristic shape, instead mode shape. This could be due to inadequate excitation of the modes from one reference and insufficient measurement DOFs. From

this inference it was concluded to perform Multi Input Multi Output modal testing for precise mobility, FRF, measurements.

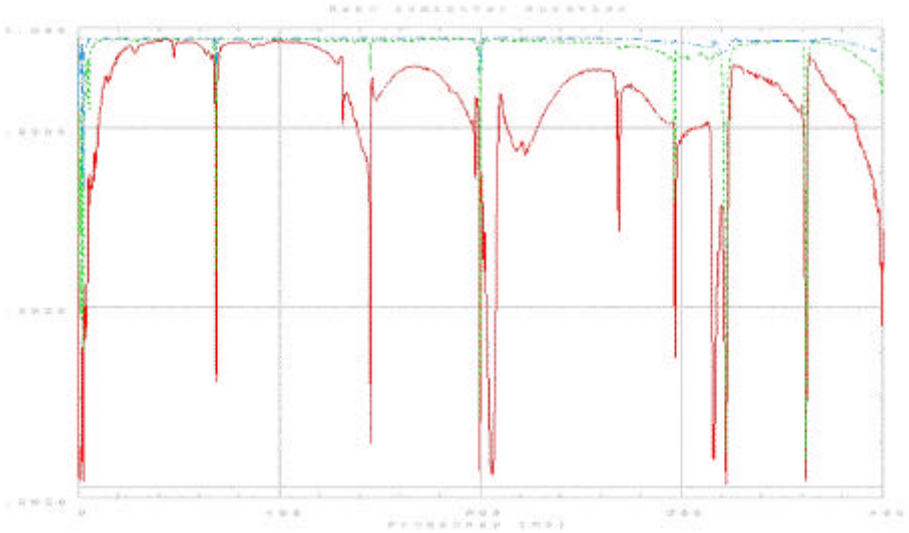

Figure 6.8, Multivariate MIF.

Table 6.2, Results from preliminary survey (core with headers & side plates).

Mode shapes	Mode	Mode shapes	Mode(core
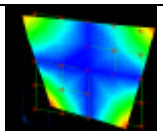	#1, 68.60 Hz	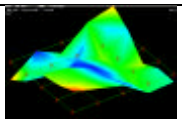	#2, 145.47 Hz
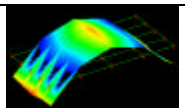	#3, 199.82 Hz	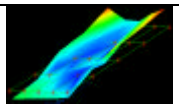	#4, 206.75 Hz
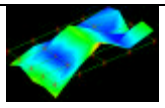	#5, 296.88 Hz	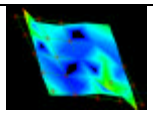	#6, 316.05 Hz
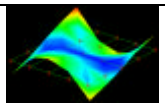	#7, 322.30 Hz		

6.4 Multi Input Multi Output Testing (MIMO)

A better energy distribution through out the structure is provided by skewed positioning of two shakers at the respective reference points, i.e. one on each bottom corner of the test structure (refer Figure 6.3). The chosen excitation signal is Burst random, a non deterministic signal, that satisfies the periodicity requirement of the FFT process. Here the signal is used only during a portion of data capture and terminated for the rest of the measurement time making the response signal to decay during this time. Hence, there is no leakage and no windows are used. The measurement settings are shown in Table 6.3.

Four scans of measurements are made by considering twice times 8 MP followed by 4 and 5 to cover 25 MP in all X, Y, Z directions, totally measuring 150 FRFs (75 FRFs for each reference). During last two scans of measurement the unused accelerometers where placed in the structure so as to have consistency in added mass. Though care was ensured the measurements had a negligible mass loading effect which is inferred from Figure 6.9. The obtained arbitrary multiple coherence, refer Figure 6.11, has unity, which shows good frequency resolution and signal to noise ratio. Similarly, the multiple coherence obtained for the second phase of measurement on test structure core without headers and side plates, is shown in Figure 6.12.

Table 6.3, Measurement settings for shaker testing.

Parameters	Settings
Number of frequency lines	1601
Frequency Span	800 Hz
Measurement time /block	2 sec
Frequency resolution	0.5 Hz
Trigger settings	Source signal
Number of Averages	40
Excitation signal	Burst random (no window; 70% duration)
Force level	0.42144

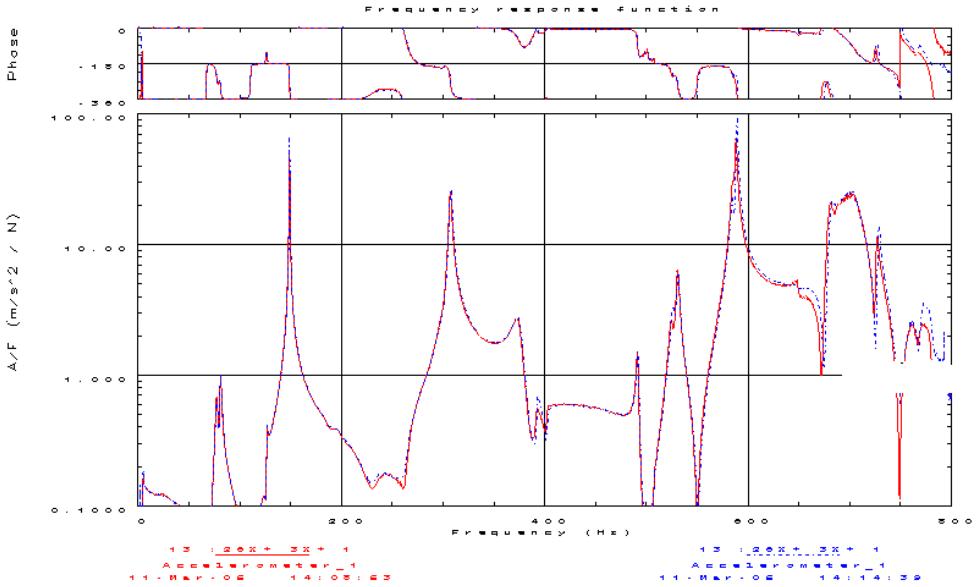

Figure 6.9, Overlaid FRF shows effect of mass loading due to 9 accelerometers.

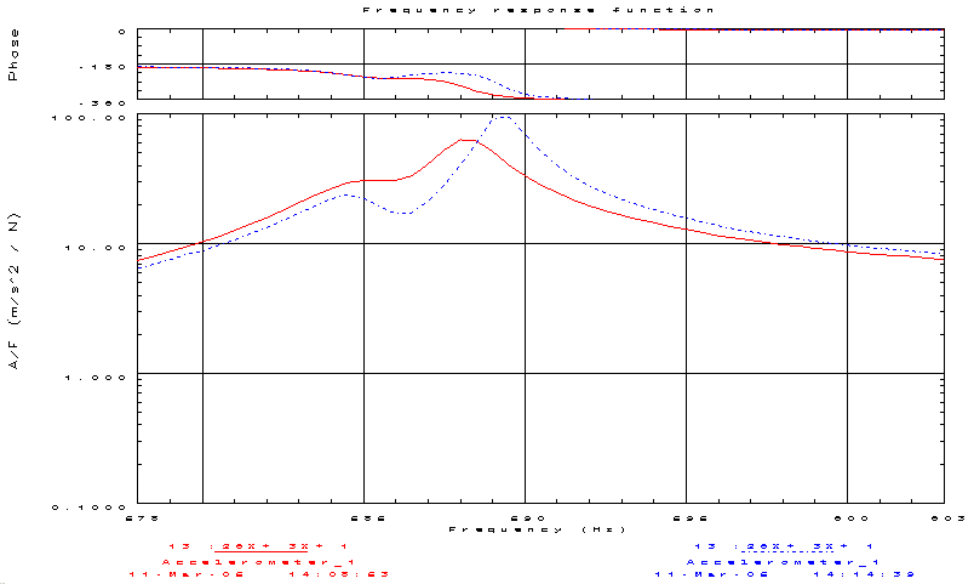

Figure 6.10, Zoom view on mass loading.

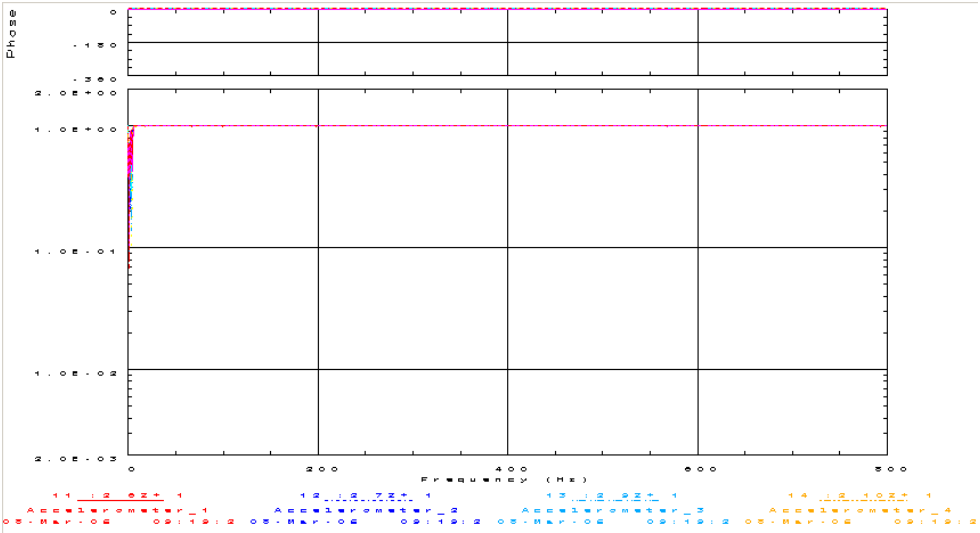

Figure 6.11, Arbitrary multiple coherence from test structure core with headers and side plates.

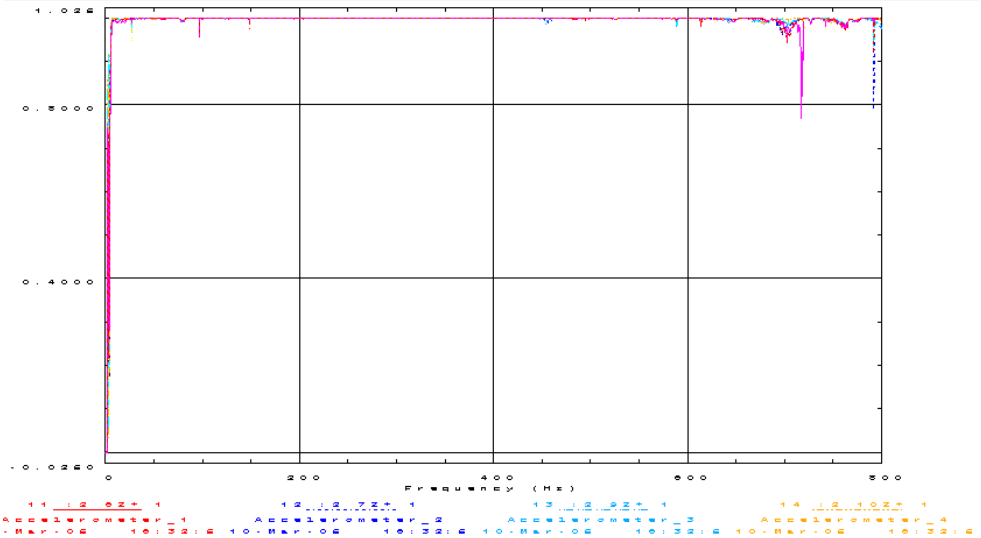

Figure 6.12, Arbitrary multiple coherence from test structure core without headers and side plates.

7 Modal parameter extraction

In the previous chapter, techniques used for making mobility measurement for analysis where seen. Having acquired satisfied measurement data, FRF matrix ([H]) elements, the next major step of the process is the use of parameter estimation techniques; curve fitting to identify the modal parameters. The data's from MIMO testing for all principle directions consist of 75 rows and 2 columns from which modal parameters where extracted by the curve fitting algorithm, Polyreference Time Domain Method (PTDM). This is an extension of Least Square Complex Exponential method to a MIMO version that includes information not only from several output locations, but also from several input reference points on the test structure. In this method all the available FRFs are processed simultaneously from various excitation and response locations. By processing data in this way it automatically averages out small variations and yields a consistent and unique set of modal properties. Parameter extraction using I-DEAS test software, modal task, is a straight forward procedure. The key steps are as follows [12].

- Generating MIF.
- Generating stability diagram
- Generating residues
- Generating mode shapes
- Building MAC matrix

7.1 Generating MIF

The multivariate MIF is selected after selecting the polyreference method in the modal task. MIF assists in selecting poles, so as to find the best assumption for modal order. Mode Indication Function (MIF) is normally a real-valued frequency domain function that exhibits local minima at the natural frequencies of the real normal modes. One mode indication function is plotted for each reference in the measured data. The primary mode indication function will exhibit local minima for each natural

frequency of the tested structure. The secondary mode indication function will exhibit local minima at repeated or pseudorepeated roots of order 2 or more. Additional mode indication functions yield local minima for successively higher orders of repeated or pseudorepeated roots. To evaluate this possibility a minimization problem is formulated as follows [9].

$$\lambda = \min_{\|F\|=1} \frac{\{F\}^T [H_{Real}]^T [H_{Real}] \{F\}}{\{F\}^T \left([H_{Real}]^T [H_{Real}] + [H_{Imag}]^T [H_{Imag}] \right) \{F\}} \qquad (7.1)$$

The minimization problem is similar to a Rayleigh quotient, and the solution is found by finding the smallest eigenvalue λ_{min} and the corresponding eigenvector $\{F\}_{min}$ of the eigenproblem given below.

$$\{F\} [H_{Real}]^T [H_{Real}] = \lambda \left([H_{Real}]^T [H_{Real}] + [H_{Imag}]^T [H_{Imag}] \right) \{F\} \qquad (7.2)$$

Equation (7.2) is formulated at each frequency in the frequency range of interest. The obtained MIF for both case of the test structure is shown in Figure 7.1 and Figure 7.2 where primary and secondary MIFs correspond to red and blue plot, respectively.

Note that there is a difference in Y-axis scale in the MIFs shown below.

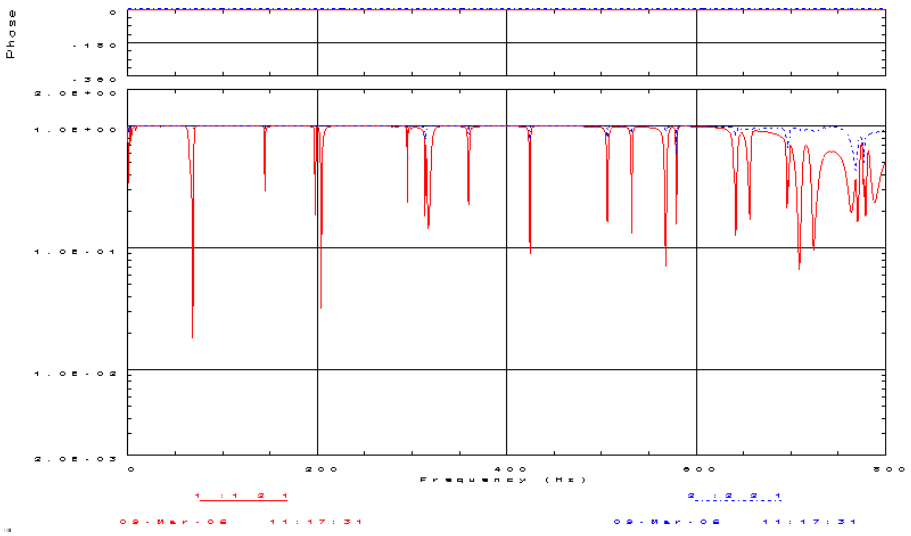

Figure 7.1, MIF - test structure core with headers and side plates.

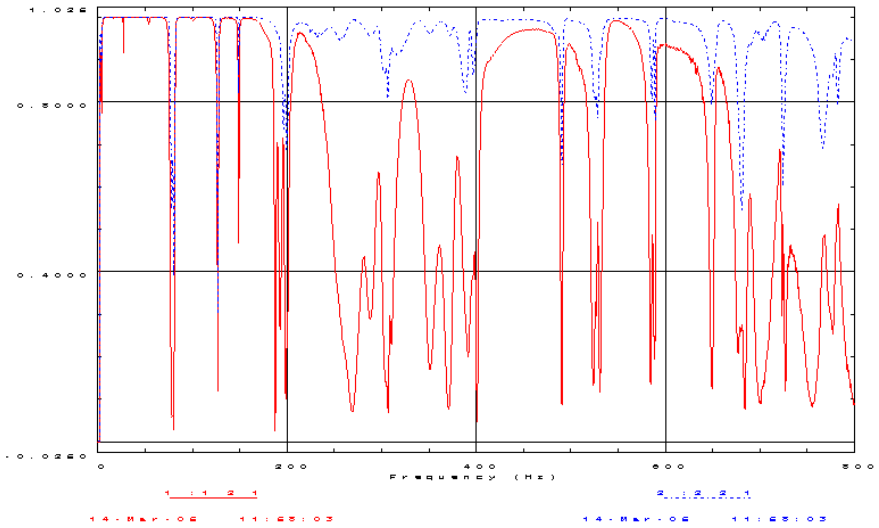

Figure 7.2, MIF - test structure core without headers and side plates.

7.2 Generating stability diagram

The reference points are selected in the model geometry description of the test structure (refer Figure 6.3). To generate stability diagram we build a correlation matrix which is an intermediate step in the parameter estimation algorithm. With the given input matrix size the polyrefernce matrix is iteratively computed. By default, the matrix routine calculates the Mode Confidence Factor (MCF) for each pole. An MCF value close to 1.0 indicates a pole that most likely represents a mode. A value close to zero represents noise or computational pole. The matrix routine automatically calculates the poles for the various pole counts up to the specified matrix size. With this the stability diagram is generated for both case of test structure, refer Figure 7.3 & Figure *7.4*, showing all the poles, which have MCF above the specified threshold value. The stability diagram involves tracking the estimates of frequency, damping, and possibly modal participation factors as a function of modal order.

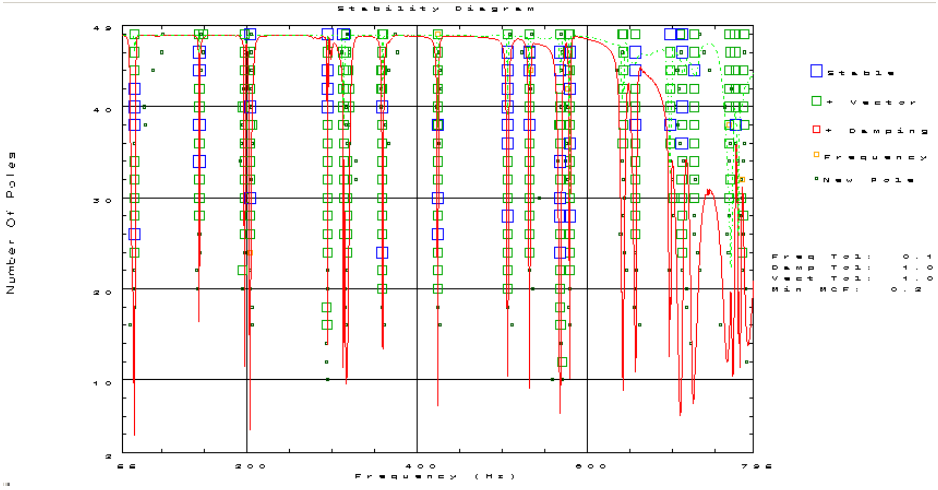

Figure 7.3, Overlaid stability plot with MIF - test structure core with headers and side plates.

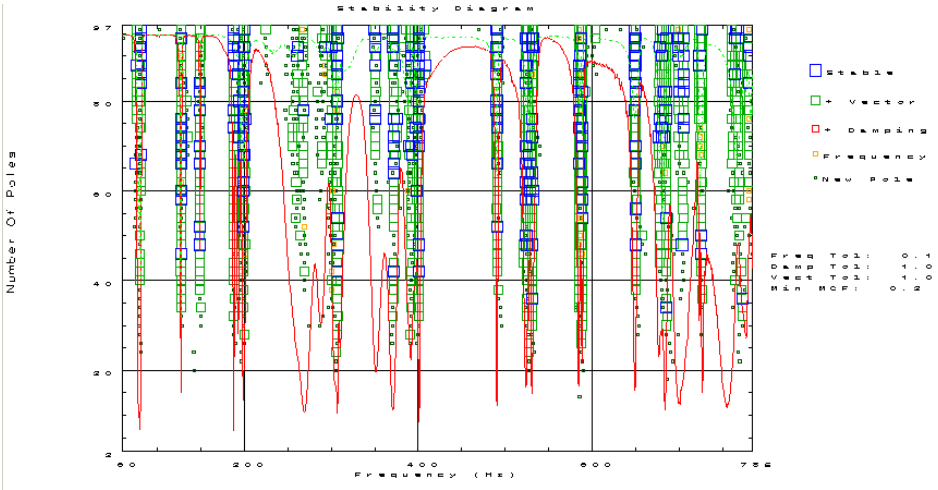

Figure 7.4, Overlaid stability plot with MIF - test structure core without headers and side plates.

7.3 Generating residues

The algorithm PTDM uses time domain equivalent, impulse response function, computed by taking inverse FFT of the measured function.

Theoretically this contains information that is represented by the characteristic equation, the modal frequencies and damping. Here the solution procedure uses all the references in the estimation process simultaneously giving the global modal parameter set. The software works by generating stability diagram by giving suitable frequency range as input. Now we overlay the MIF on the stability diagram and the stable poles (blue squares) are picked for each mode indicated by the MIF. Residues are generated for this modal parameter set. Here the software prompts the user for a specific measurement point and synthesises the FRF for the specified point. If the synthesized FRF is acceptable the next step is to generate mode shapes, else the procedure is repeated by changing the frequency range.

7.4 Generating mode shapes

Mode shapes are generated using the Frequency Polyreference method. The extracted mode shapes are viewed and animated in the post processing task. The results for both cases of test structure are shown in Table 7.1 and Table *7.2*.

Table 7.1, Mode shapes- test structure core with headers & side plates.

Mode shapes	Resonance frequency [Hz]	Relative damping [%]
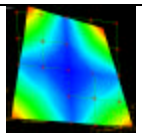	#1, 68.27	1.55
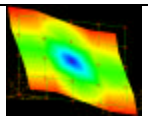	#2, 144.7	0.21
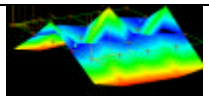	#3, 197.79	0.12
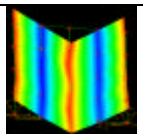	#4, 205.63	2.19

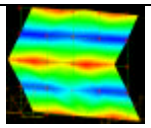	#5, 294.91	0.06
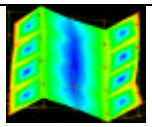	#6, 313.71	0.12
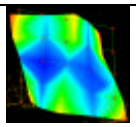	#7, 320.06	0.76
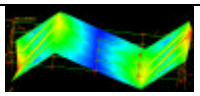	#8, 359.67	0.12
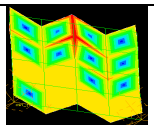	#9, 424.44	1.46
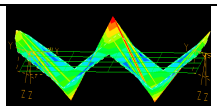	10, 506.36	0.09
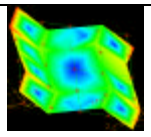	#11, 532.02	0.11
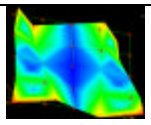	#12, 567.87	0.23
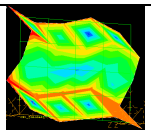	#13, 579.19	0.07
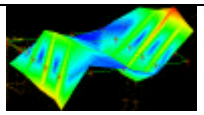	#14, 641.7	0.13
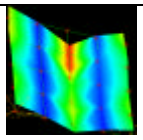	#15, 656.42	0.17

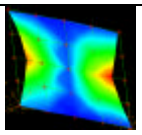	#16, 696.88	0.13
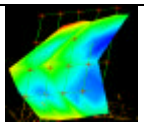	#17, 710.69	0.44
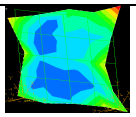	#18, 725.51	0.63
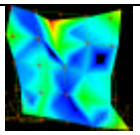	#19, 766.56	0.88
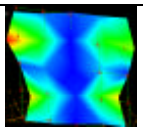	#20, 773.64	0.36
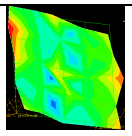	#21, 783.39	0.81

Table 7.2, Mode shapes- test structure core without headers & side plates.

Mode shapes	Resonance frequency [Hz]	Relative damping [%]
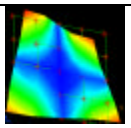	#1, 80.72	1.28
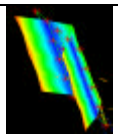	#2, 126.81	0.39
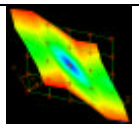	#3, 148.76	0.11
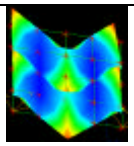	#4, 187.61	0.55
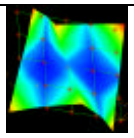	#5, 200.48	0.92
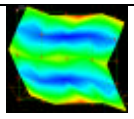	#6, 307.75	1.34
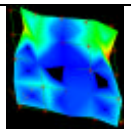	#7, 350.75	2.6
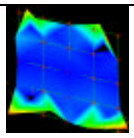	#8, 372.5	1.29
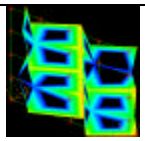	#9, 401.08	0.40

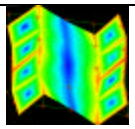	#10, 491.16	0.23
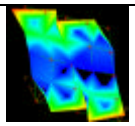	#11, 523.57	0.44
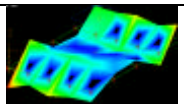	#12, 530.82	0.28
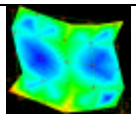	#13, 584.74	0.20
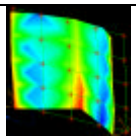	#14, 650.64	0.29
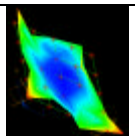	#15, 677.34	0.45
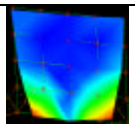	#16, 705.16	1.2
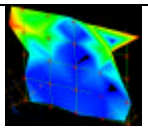	#17, 723.45	0.21
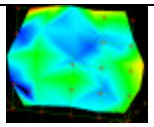	#18, 765.23	2.48

7.5 Building MAC matrix

To verify the curve fitting, for quality assessment, MAC matrix is built. Here the mode shape file is chosen twice, one time for rows and the second time for columns, so that two different mode shape files are compared. MAC is the measure of the correlation coefficient between each mode shape in a set of modes with those of another set. A MAC value of zero means there is no correlation, whereas a MAC value of unity means the modes are identical. MAC matrices resulting from both test structures show diagonal elements equal to unity, which represents good correlation (refer Figure 7.5 & Figure 7.6).

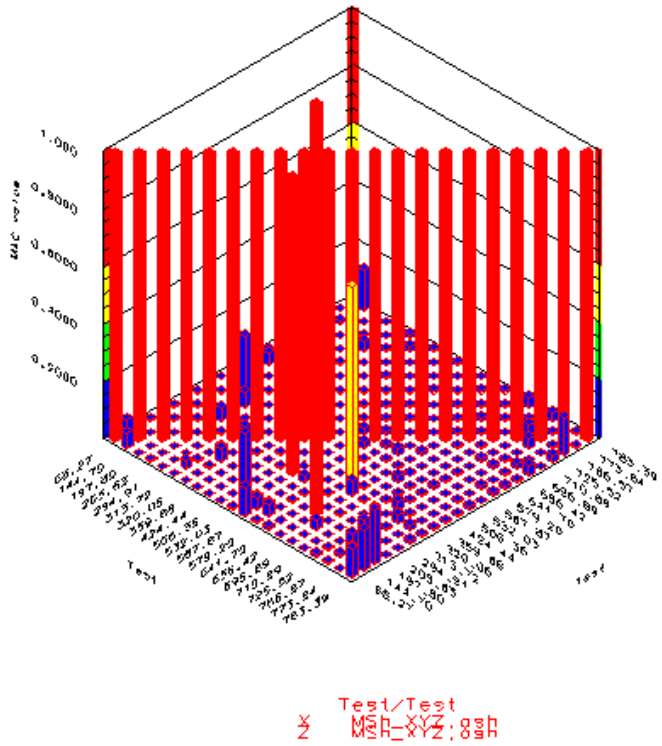

Figure 7.5, MAC - test structure core with headers & side plates.

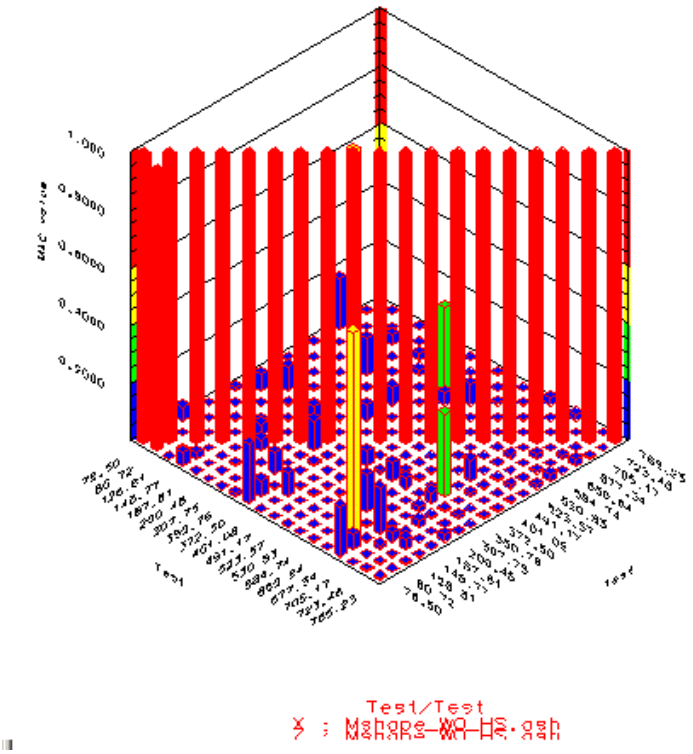

Figure 7.6, MAC - test structure core without headers & side plates.

8 Model Validation

In PD process driven by analytical simulation a theoretical model should be reliable enough for better estimation of products behaviour. Here we *reconcile* the FE model to the obtained modal characteristics, namely natural frequencies and mode shapes, from test data. This reconciliation process is often referred to as model correlation where we update the verified FE model. As mentioned, the FE-model is correlated with the tube bending modes of first order, including the first six modes. A model can be said a valid FE model if it satisfies its degree of acceptance. Due to time constraint only the FE model of the core alone is considered.

8.1 Model verification

Model verification is an important step in the process of model validation. In this step, the model is *debugged* to verify that it is modelled according to the initial requirement, i.e. closer in acceptance to the behaviour of the physical model. In the viewpoint of model validation, model verification should provide a verified model, which can be updated to match the test data only by modifying the parameters of the model [11]. The comparison of resonance frequencies from the initial FE model and test data are tabulated in Table 8.1.

Table 8.1, Comparison of Test Vs Initial FE model data's

Test Data	Mode, Resonance frequency	Initial FE-model	Mode, Resonance frequency	Difference
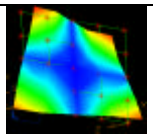	#1, 1 st Torsion 80.72 Hz	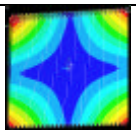	#1, 1 st Torsion 50.69 Hz	45.7%
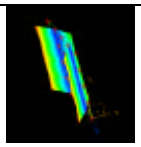	#2, Bending Y 126.81 Hz	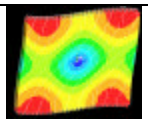	#2, Shear YZ 151.74 Hz	2%
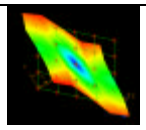	#3, Shear YZ 148.77 Hz	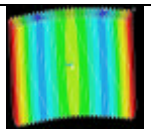	#3, Bending Y 188.60 Hz	39%
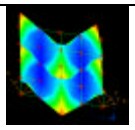	#4, Bending X (Header) 187.61 Hz	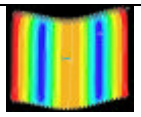	#4, Bending X (Header) 197.46 Hz	5%
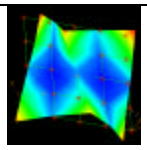	#5, 2 nd Torsion 200.48 Hz	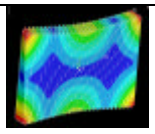	#5, 2 nd Torsion 201.83 Hz	0.7%
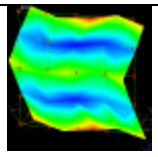	#6, Bending X (Side plate) 307.75 Hz	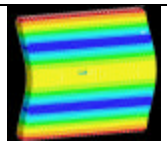	#6, Bending X (Side plate) 266.90 Hz	14.2%
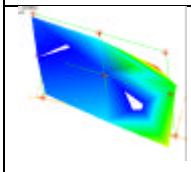	#19, Bending Z 853.39 Hz	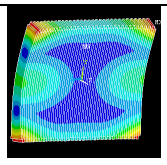	#21, Bending Z 767.7 Hz	10.6%
Coordinate system directions		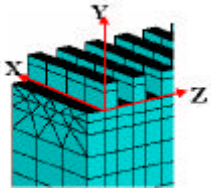		

As inferred in the above table (Table 8.1) the results are incompatible with test data. The initial FE model is checked for convergence error where the detailed description of the FE model of fin is verified with different mesh density from which orthotropic material properties where extracted, as discussed in chapter 3. The results showed that the model is converged and there is no considerable influence on the natural frequencies with modified parameters for fin. It is necessary that the model needs to be checked for configuration error. Here the prediction is that the simplified representation of tube in core would misrepresent the key features as they are supposed to be. So a design change is been called for where the tube is modelled in oval shape, for better representation of the physical model, using shell elements, leaving only the turbolator and fin simplified (homogenised). The design change in the initial FE-model is seen in Figure 8.1 (the coordinate system shown represents the elements coordinate system).

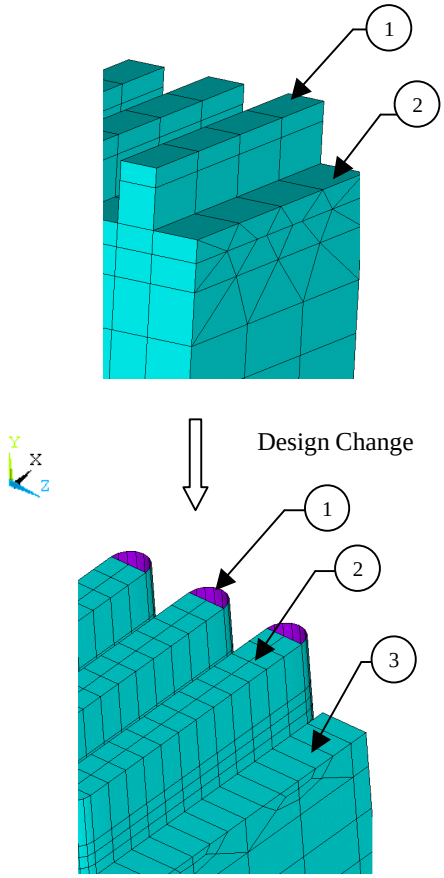

INITIAL FE-MODEL

1. Simplified representation of Tube +Turbolator (homogenised)
2. Simplified representation of Fin (homogenised)

MODIFIED FE-MODEL

1. Tube, oval shape, modelled with Shell element
2. Simplified representation of Turbolator (homogenised)
3. Simplified representation of Fin (homogenised)

Figure 8.1, Design change in initial FE-model.

This modified FE model comprises of two sets of orthotropic properties for turbolators and fins along with isotropic property defined for tubes, totally 23 material parameters including mass densities. A simple parameter study is performed by incrementing, separately, the 18 orthotropic parameters (turbolator and fin) by 50 %. The results where examined, which revealed that Young's modulus Ez of turbolator has a considerable effect that brings all targeted modes in better agreement with the test data. The results from the design change and the 50% increment of Ez (turbolator) is shown in Table 8.2.

Table 8.2, Results of design change & 50% increment of Turbolator Ez.

Modified FE-model	Resonance frequency [Hz]	50% Increment of Turbolator Ez	Resonance frequency [Hz]
#1,1 st Torsion	79.82	#1,1 st Torsion	80.482
#2,Bending Y	94.55	#2,Bending Y	123.26
#3,Shear YZ	154.7	#3,Shear YZ	155.03
#4,2 nd Torsion	183.9	#4,2 nd Torsion	199.7
#5,Bending X (Header)	195	#5,Bending X (Header)	199.7
#6,Bending X (Side plate)	303.4	#6,Bending X (Side plate)	303.46
#26,Bending Z	793.7	#23,Bending Z	794.06

It is inferred from the results (refer Table 8.2) that the FE data, when on incrementing parameter Ez of turbolator, is compatible with test data and the modified FE-model can be said as a *Verified FE-model*. The verified model is also checked for mass property where it has +3% errors on comparing with physical model.

8.2 Model updating

Model updating in model validation is an iterative process where the parameter values of a verified FE model are corrected, tuned, to bring the FE model prediction into better agreement with test data. The results of the parameter study are used so as to identify the appropriate parameters to be tuned.

While the 50% increment of turbolator Ez is kept constant, further tuning of material parameters is carried to find the right combination of parameters. It is considered important to get a better correlation of Bending Z mode, which was accomplished by incrementing the parameter Ey of turbolator by 175%. The comparison of resonance frequencies of the updated FE-model

and test data is shown in the Table 8.3. The variation in percent from the original extracted orthotropic material properties of turbolator and fin to get the correlated FE-model of core are shown in Table 8.4.

Table 8.3, Comparison of Test Vs Updated FE model data's.

Test Data	Mode, Resonance frequency	Updated FE-model	Mode, Resonance frequency	Difference
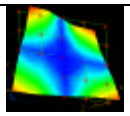	#1, 1st Torsion 80.72 Hz	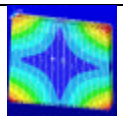	#1, 1st Torsion 80.09 Hz	0.8%
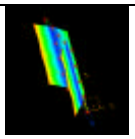	#2, Bending Y 126.81 Hz	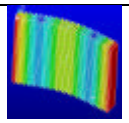	#2, Bending Y 127.78 Hz	0.8%
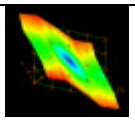	#3, Shear YZ 148.77 Hz	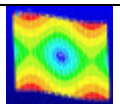	#3, Shear YZ 146.63 Hz	1.4%
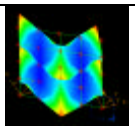	#4, Bending X (Header) 187.61 Hz	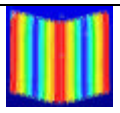	#4, Bending X (Header) 189.32 Hz	0.9%
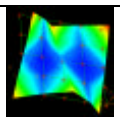	#5, 2 nd Torsion 200.48 Hz	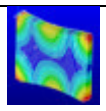	#5, 2 nd Torsion 201.78 Hz	0.6%
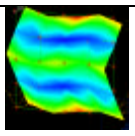	#6, Bending X (Side plate) 307.75 Hz	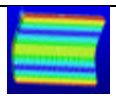	#8, Bending X (Side plate) 294.56 Hz	4.3%
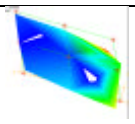	#19, Bending Z 853.39 Hz	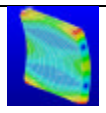	#27, Bending Z 841.58 Hz	1.4%

Table 8.4, Modification in percent of material properties from original value.

Modified Material properties	Increment from original value	Decrement from original value
Turbolator E_y	175%	-
Turbolator E_z	50%	-
Turbolator G_{yz}	5%	-
Fin G_{yz}	-	10%
Fin E_z	5%	-

9 Conclusion and discussions

Correlating a FE-model data on comparing its resonance frequencies with corresponding modal test data of the charge air cooler core is the subject of this thesis work. Due to time constraint only the subcomponent core without headers and side plates were correlated. However, EMA was performed on the component core with headers and side plates. The suitable measurement parameters were also specified.

The comparison between resonance frequencies of the updated FE-model and modal testing result shows a good agreement and satisfies the level of acceptance. Hence the updated FE-model is said as a valid FE-model.

It is inferred in the table (8.3) that there are extra modes in the updated FE-model results, which is quite common. As an effect of this, mode #8 and mode #27 of the FE-model data is correlated with the corresponding mode #6 and mode #19 of the test data.

The experimental investigation shows that in order to acquire good and understandable mode shapes, the structure requires MIMO treatment with response points covering all three principle directions. It is also inferred that the structure is linear and lightly damped.

The FE-model verification results showed that simplifying tubes (homogenisation) lead to misrepresentation and incompatible results. If possible, tubes should be modelled with shell or solid elements of isotropic material properties representing its actual geometry.

The material parameter variation in the FE-model updating showed that, only the turbolator material properties Ez and Ey had a significant influence on resonance frequencies of the interested modes. Here the prediction is that the realistic description of the FE-model of turbolator used for homogenisation has incorrect elastic behaviour. Hence some changes in the realistic description of turbolator FE-model are required. For example the turbolator could be modelled with solid elements instead of shell elements.

10 References

1 Broman, G., Jönsson, A. & Hermann, M., (1999), 'Modeling Flexible Bellows by Standard Beam Finite Element', research report 12/99.

2 Ragab, A.R., Bayoumi, S.E., (1999), 'Engineering Solid Mechanics', CRC Press LLC, Florida 33431.

3 ANSYS manual guide,(Chapter 2) 'Structural Fundamentals'.

4 Planel, O., Holmgren, K., Brisson, S., Thionnet, A., (03/2003), 'Modelling of a Brazed Exchanger Core by Homogenisation Method', Project EHA002 – Fatigue in vibration.

5 Avitabile, P., (2000), Modal Space: Back to Basics, Experimental Techniques, 24, No.5, pp. 15-16.

6 Maia, Silva, He, Lieven, Lin, Skingle, To and Urgueira (1997) 'Theoritical and Experimental Modal Analysis', Research Studies Press LTD., 1997.

7 Brandt, A. (2001), 'Introductory Noise and Vibration Analysis', Saven Edutech AB, Täby, Sweden.

8 Ahlin, K., Brandt, A., (2001), 'Experimental Modal Analysis in Practice', Saven Edutech AB, Täby, Sweden.

9 Allemang, R., Brown, D., (Chapter 16), Experimental Modal Analysis, Structural Dynamics Research Laboratory, University of Cincinnati, Ohio.

10 Allemang, R. (1998), Vibrations: Analytical and Experimental Modal Analysis, Class notes, University of Cincinnati, Ohio.

11 Chen, G., Ewins, D.J., Verification of FE Models for Model Updating, Dynamic Section, Mechanical Engineering Department, Imperial college of science, U.K.

12 I-DEAS manual guide, 'Modal analysis'.

A. Verification of extracted orthotropic material properties

Table (A.1), Verification of extracted orthotropic material properties of fin.

Compliance matrix checked for positive definite = $2.20*10^{-1} > 0$		
Poisson's ratio	Calculated using ANSYS results	Calculated using symmetry condition
PR_{yx}	$4.27*10^{-5}$	$4.27*10^{-5}$
PR_{zx}	$1.00*10^{-2}$	$1.00*10^{-2}$
PR_{zy}	$7.59*10^{1}$	$7.59*10^{1}$

Table (A.2), Verification of extracted orthotropic material properties of Tube + Turbolator.

Compliance matrix checked for positive definite = $9.43*10^{-1} > 0$		
Poisson's ratio	Calculated using ANSYS results	Calculated using symmetry condition
PR_{yx}	$2.43*10^{-1}$	$2.43*10^{-1}$
PR_{zx}	$2.14*10^{-3}$	$2.14*10^{-3}$
PR_{zy}	$4.09*10^{-4}$	$4.07*10^{-4}$

Table (A.3), Verification of extracted orthotropic material properties of Turbolator.

Compliance matrix checked for positive definite = $5.68*10^{-1} > 0$		
Poisson's ratio	Calculated using ANSYS results	Calculated using symmetry condition
PR_{yx}	1.42	1.42
PR_{zx}	$2.76*10^{1}$	$2.70*10^{1}$
PR_{zy}	$2.60*10^{-3}$	$2.60*10^{-3}$

* It inferred that there is a small variation in the verification of Poisson's ratio PR_{zy} refer table (A.2) and PR_{zx} refer table (A.3), which is considered negligible.

B. CD - Attachments

The following files are attached in the CD:

1.) “Boundary conditions.doc” - contains the boundary conditions applied to extract orthotropic material properties using homogenisation technique.

2.) “Fin_prop.xls”, “Tube_prop.xls”, “Tube+Turbolator_prop.xls” - show the ANSYS output and computed orthotropic material properties of the Fin, Tube + Turbolator and Turbolator.

3.) “Core_FE-model_bynode.txt” - macro that builds the FE-model of core.

Department of Mechanical Engineering, Master's Degree Programme
Blekinge Institute of Technology, Campus Gräsvik
SE-371 79 Karlskrona, SWEDEN

Telephone: +46 455-38 55 10
Fax: +46 455-38 55 07
E-mail: ansel.berghuvud@bth.se